Journal of Lasers in Medical Sciences

J Lasers Med Sci 2026;17:e50021

Original Article

http://journals.sbmu.ac.ir/jlms

doi:10.34172/jlms.50021

# Effects of Photobiomodulation on Ventilatory Mechanics and Inflammatory Response in a Rat Model of Acute Lung Injury

**Rafaella Rocha Figueiredo[1], Gabrielly Santos Pereira[1], Laura Pereira Generoso[1], João Eduardo de Araújo[2], Josie Resende Torres da Silva[1], Marcelo Lourenço da Silva[1*]**

[1]Laboratory of Neuroscience, Neuromodulation and Study of Pain (LANNED), Federal University of Alfenas (UNIFAL-MG), Alfenas, MG, Brazil

[2]Department of Health Sciences, Ribeirão Preto Medical School, University of São Paulo, São Paulo, Brazil

***Correspondence to**
Marcelo Lourenço da Silva,
Email: marcelo.lourenco@unifal-mg.edu.br

**Received:** August 22, 2025
**Accepted:** December 6, 2025
**ePublished:** May 16, 2026

## Abstract

**Introduction:** Acute Lung Injury (ALI) and Acute Respiratory Distress Syndrome (ARDS) are life-threatening inflammatory conditions characterized by neutrophil recruitment, cytokine storm, and disruption of ventilatory mechanics. Despite advances in supportive care, effective pharmacological therapies remain limited. Photobiomodulation (PBM), using different light spectra, including LED and low-level laser therapy (LLLT), has shown potential anti-inflammatory and tissue-regenerative effects. However, the specific impact of PBM on acute lung inflammation is not fully established.

**Methods:** This experimental study involved 288 male Wistar rats subjected to tracheal instillation of Escherichia coli lipopolysaccharide (LPS) to induce acute lung injury. Animals were allocated to control and treatment groups receiving 430 nm LED, 660 nm red laser, or 808 nm infrared laser. After 24 hours, ventilatory mechanics (resistance, viscosity, elastance, and hysteresivity) were assessed through mechanical ventilation. Lung tissue was analyzed for myeloperoxidase (MPO) activity, cytokine expression (TNF-α, IL-1β, IL-6, IL-10) by RT-qPCR, and histological alterations.

**Results:** Among the phototherapies, the 660 nm red laser was the only intervention capable of significantly reducing all parameters of ventilatory mechanics, MPO activity, and inflammatory cytokines, with histological evidence of attenuated neutrophil infiltration, reduced alveolar wall thickening, and decreased pulmonary edema. The 430 nm LED attenuated only selective cytokines without histological or mechanical benefits, while the 808 nm infrared laser reduced TNF-α and IL-6 with partial histological improvement but no effect on lung mechanics.

**Conclusion:** PBM with a 660 nm red laser effectively modulated the inflammatory cascade in LPS-induced ALI, reducing the cytokine storm and improving ventilatory function with histological evidence of lung protection. These findings highlight PBM as a potential adjuvant therapy for acute lung inflammation.

**Keywords:** Photobiomodulation, Low-level laser therapy, Lung injury, Acute respiratory distress syndrome, Inflammation

## Introduction

Acute Lung Injury (ALI) and its severe manifestation, Acute Respiratory Distress Syndrome (ARDS), are critical conditions characterized by diffuse damage to the alveolar–capillary membrane, leading to impaired gas exchange, pulmonary edema, and progressive respiratory failure.[1,2] Although the term "lung injury" is less frequently used in clinical practice, it remains widely applied in preclinical research, where no single animal model fully replicates the complexity of ARDS.[3] Lipopolysaccharide (LPS) instillation is among the most established experimental models, simulating pneumonia-induced injury and reproducing the rapid onset of inflammation and structural disruption of lung tissue observed in humans.[4,5] This model is marked by early neutrophil accumulation within the alveolar and interstitial spaces, thickening and edema of the alveolar wall, and subsequent parenchymal damage.[6]

The inflammatory cascade triggered by LPS plays a central role in ALI/ARDS pathogenesis. Macrophages, representing the majority of immune cells in the alveolar space, initiate the response by releasing pro-inflammatory mediators that drive neutrophil recruitment and activation.[7] While essential for host defense, excessive

**Please cite this article as follows:** Figueiredo RR, Pereira GS, Generoso LP, Araújo JEd, Silva JRTd, Silva MLd. Effects of photobiomodulation on ventilatory mechanics and inflammatory response in a rat model of acute lung injury. J Lasers Med Sci 2026;17:e50021. doi:10.34172/jlms.50021

neutrophil activity amplifies tissue injury through the release of proteases, elastases, and reactive oxygen species, further compromising epithelial and endothelial integrity.[8-10] Damage to the alveolar epithelium disrupts barrier function, facilitates protein leakage, and contributes to pulmonary edema, a hallmark of ALI/ARDS.[2] Despite progress in supportive therapies, including mechanical ventilation and pharmacological attempts to mitigate the "cytokine storm," effective targeted interventions remain lacking.[8-11]

Photobiomodulation (PBM) has emerged as a promising adjunctive strategy due to its anti-inflammatory, regenerative, and immunomodulatory effects. Advances in light-based technologies have demonstrated that specific wavelengths—such as violet/blue light emitted by LEDs and red or infrared light delivered by low-level laser therapy (LLLT)—can influence biological responses at the cellular and tissue levels.[12] Experimental evidence suggests PBM may attenuate inflammatory cell infiltration, downregulate cytokine production, and promote tissue repair, although outcomes depend critically on parameters such as wavelength, fluence, and exposure time.[13-17] Notably, red light exhibits favorable penetration into lung tissue, whereas infrared light is often associated with analgesic effects.[15,17]

Given these properties, PBM could serve as an adjuvant or alternative therapy to reduce lung inflammation and improve prognosis in ALI/ARDS.[18] Mechanistically, PBM is believed to act primarily through the absorption of photons by mitochondrial chromophores, especially cytochrome c oxidase, leading to enhanced electron transport, increased ATP synthesis, and secondary modulation of reactive oxygen species and inflammatory signaling pathways.[12-17] Animal studies are essential to establish its mechanisms and therapeutic potential. We hypothesized that PBM would exert protective effects in LPS-induced ALI by attenuating inflammation and improving ventilatory function, and that these effects would be wavelength-dependent, with a 660 nm red laser providing the most comprehensive benefit. Therefore, the present study aimed to evaluate the effects of PBM at different wavelengths on inflammatory cell recruitment, cytokine expression, myeloperoxidase (MPO) activity, ventilatory mechanics, and histopathological changes in a rat model of LPS-induced lung injury.

## Methods

### *Animals*

We used 288 male Wistar rats, aged 7–8 weeks and weighing 250–300 g. Animals were housed in the Department of Physiotherapy, Central Bioterium at the Federal University of Alfenas (UNIFAL-MG). They were maintained in acrylic cages under controlled environmental conditions: a temperature of 18–21 °C, a relative humidity of 55–60%, and a 12 h light/dark cycle. Food and water were provided ad libitum. All procedures complied with institutional and national ethical standards for animal research and were approved under registration number 21/2020.

### *Experimental Groups*

Animals were randomly assigned to twelve experimental groups (n = 24 per group, total = 288 rats): vehicle/sham, vehicle/LED 430 nm, vehicle/laser 660 nm, vehicle/laser 808 nm, vehicle/vehicle, vehicle/dexamethasone (DEXA), LPS/sham, LPS/LED 430 nm, LPS/laser 660 nm, LPS/laser 808 nm, LPS/vehicle, and LPS/DEXA.

### *Anesthesia and Induction of Lung Injury*

Rats were anesthetized intraperitoneally with ketamine (100 mg/kg; Ketamine®) and xylazine (10 mg/kg; Dopaser®). Following trichotomy and asepsis of the cervical region, a midline skin incision was performed, the muscles were retracted, and the trachea was exposed. Acute lung injury was induced by intratracheal instillation of Escherichia coli lipopolysaccharide (LPS; Sigma, 2 mg/kg) or vehicle (PBS), using a 27 G needle inserted between tracheal cartilage rings. The cervical incision was then closed with a 4.0 silk suture. During anesthetic recovery, external heating was provided to prevent hypothermia. Positive control animals received dexamethasone (1 mg/kg, orally) one hour before LPS instillation, while sham groups received vehicle solution (0.5% methylcellulose/0.2% Tween 80, orally).[19]

### *Photobiomodulation Protocol*

One hour after LPS or PBS instillation, the animals were subjected to photobiomodulation. Treatments were applied over the skin at the sternum, close to the anatomical projection of the right upper lung lobe. The following irradiation protocols were used: 660 nm red laser (Therapy EC, DMC, Brazil): emission power of 100 mW, fluence of 9 J/cm², exposure time of 90 s, and spot size of 0.06 cm²; 808 nm infrared laser (Therapy EC, DMC, Brazil): parameters identical to the 660 nm red laser; 430 nm LED (D-2000, DMC, Brazil): emission power of 900 mW, continuous mode, exposure time of 30 s, and spot size of 1.0 cm². The selected wavelengths (430, 660, and 808 nm) were chosen to represent distinct regions of the optical window with known biological relevance: 430 nm (blue) for superficial photochemical and antimicrobial interactions, 660 nm (red) for optimal absorption by mitochondrial cytochrome c oxidase, and 808 nm (infrared) for deeper tissue penetration and modulation of inflammatory signaling.[15–17, 20, 21]

The laser dose was selected to target a radiant exposure within the effective range reported for pulmonary PBM in rodent ALI/ARDS models, which commonly use red/near-infrared wavelengths and radiant exposures on the order of 7.5–30 J/cm², balancing the biphasic dose–response

and the optical penetration window in lung tissue.[15,17,22-24] For the 430 nm LED, exposure time (30 s) was chosen to achieve a comparable energy-on-tissue within the same order of magnitude while avoiding thermal effects and accounting for the broader spectral bandwidth and lower coherence of LED emission relative to lasers.[15,17] The fluence for the 430 nm LED (27 J/cm²) was selected based on previous reports using short-wavelength PBM in inflammatory or infectious models, where higher fluence is required to compensate for the greater optical attenuation of blue light in tissue and its lower photon energy deposition per unit depth.[15,17,21] The laser protocols (660 nm and 808 nm) were designed to deliver similar total radiant energy but at higher irradiance over smaller spots, consistent with effective doses in prior pulmonary PBM studies.[23,24]

Photobiomodulation was applied one hour after LPS instillation to coincide with the early activation phase of the inflammatory cascade, preceding the peak of neutrophil recruitment and cytokine expression, which typically occurs between 2–6 hours post-LPS exposure in rodent models.[4,23,24] This time window was selected to assess PBM's ability to modulate the initial pro-inflammatory signaling rather than acting as a pre-conditioning or late rescue intervention, providing a reproducible model of early therapeutic intervention after injury induction.

### *Dosimetry and derived metrics*

660 nm laser (DMC Therapy EC): output power = 0.10 W; beam area = 0.06 cm²; time = 90s; energy = 9 J; irradiance = 1.67 W/cm²; radiant exposure (fluence) = 150 J/cm².

808 nm laser (DMC Therapy EC): nominal settings identical to the 660 nm laser; energy = 9 J; irradiance = 1.67 W/cm²; fluence = 150 J/cm².

430 nm LED (DMC D-2000): output power = 0.90 W; beam area = 1.00 cm²; time = 30s; energy = 27 J; irradiance = 0.90 W/cm²; fluence = 27 J/cm².

Although these fluences differ numerically, the protocols were designed to approximate equal total energy delivery within the effective range reported in prior pulmonary PBM studies (23, 24, 15) and to compensate for variations in coherence, divergence, and spot size among light sources.

All irradiations were delivered transcutaneously over the sternal window aligned to the projection of the right upper lung lobe.

### *Respiratory Mechanics Assessment*

Twenty-four hours after instillation, respiratory mechanics were evaluated. The animals were pre-anesthetized with xylazine (8 mg/kg, i.p.), followed by pentobarbital (40 mg/kg, i.p.) and tramadol hydrochloride (30 mg/kg, i.p.) for analgesia. A tracheostomy was performed, and a 14-G cannula was inserted and connected to a ventilator (Ventstar, RWD). Mechanical ventilation was set at the tidal volume of 6 ml/kg, respiratory rate of 120 breaths/min, and PEEP of 3.0 $cmH_2O$. Pancuronium bromide (1.0 mg/kg, i.p.) was administered for muscle relaxation. After 5 minutes, the following parameters were recorded: airway resistance (Raw), tissue viscosity (Gtis), tissue elastance (Htis), and hysteresis (η), calculated from Raw and Htis.

### *Myeloperoxidase (MPO) Activity*

Lung fragments (300–350 mg) were homogenized in 50 mM potassium phosphate buffer (pH 6.0) on ice. The homogenates were centrifuged at 12,000 g for 30 minutes at 4 °C. Pellets were resuspended in a buffer containing 5% hexadecyltrimethylammonium bromide and then subjected to three freeze–thaw cycles in dry ice and thawing at room temperature. The final thaw was followed by sonication (20–30% amplitude, 40 s, on ice). After centrifugation (10,000 g, 5 min, 4 °C), supernatants were collected for enzymatic determination of MPO activity using a colorimetric assay based on the oxidation of o-dianisidine dihydrochloride in the presence of hydrogen peroxide. Absorbance was read at 560 nm, and results were expressed as mU/g of tissue.

### *Gene Expression Analysis*

Lung tissue was homogenized, and total RNA was extracted using TRIzol (Invitrogen). RNA quality was confirmed by spectrophotometry (NanoDrop® 2000), and only samples with 260/280 ratios between 1.8 and 2.0 were used. The samples were treated with DNase to prevent genomic contamination. cDNA was synthesized using SuperScript® IV First-Strand Synthesis kit.

RT-qPCR was performed on a 7500 Real-Time PCR System (Applied Biosystems) using SYBR® Green Master Mix. Target genes included IL-1β, IL-6, IL-10, and TNF-α, with GAPDH as the reference gene. Primer sequences were as follows: IL-1β (F: 5′-TGTGAAATGCCACCTTTTGA-3′; R: 5′-GGTCAAAGGTTTGGAAGCAG-3′); IL-6 (F: 5′-CCACTTCACAAGTCGGAGGC-3′; R: 5′-CCAGGTAGAAACGGAACTCC-3′); IL-10 (F: 5′-CGGGAAGACAATAACTGCAC-3′; R: 5′-CATTTCCGATAAGGCTTGG-3′); TNF-α (F: 5′-CCACCACGCTCTTCTGTCTAC-3′; R: 5′-AGGGTCTGGGCCATAGAACT-3′); GAPDH (F: 5′-TGCACCACCAACTGCTTAGC-3′; R: 5′-GGCATGGACTGTGGTCATGAG-3′). Primers were synthesized by Síntese Biotecnologia, Brazil, and validated for amplification efficiency between 95–105%. Each reaction was performed in 8 biological replicates and 3 technical replicates.

Gene expression was quantified using the 2^−ΔΔCt method, with GAPDH as the reference (housekeeping) gene. The PBS/Sham group was used as the calibrator (control) for all comparisons, such that the relative

expression level in this group was set to 1.0. Accordingly, fold changes greater than 1.0 represent upregulation, and values less than 1.0 indicate downregulation of the respective cytokine genes relative to the baseline (PBS/Sham).

### *Histopathological Analysis*

For histology, lungs were fixed in 4% formaldehyde, embedded in paraffin, sectioned, and stained with hematoxylin and eosin (H&E). Sections were analyzed by optical microscopy to evaluate neutrophil infiltration, alveolar wall thickening, and edema. Comparisons were made among the control (PBS), LPS, LPS + DEXA, and LPS + PBM groups (430-nm LED, 660-nm laser, 808-nm laser).

### *Statistical Analysis*

For ventilatory mechanics (Raw, Gtis, Htis, and η), data were analyzed using a two-way repeated-measures ANOVA with two factors: Time (within-subjects: baseline vs. 24 hrs post-LPS) and Group (between-subjects: six levels — PBS/Sham, LPS/Sham, LPS + LED 430 nm, LPS + Laser 660 nm, LPS + Laser 808 nm, LPS + Dexamethasone).

Greenhouse–Geisser corrections were applied when necessary. Bonferroni post hoc tests were performed for pairwise comparisons, primarily contrasting each LPS-treated group with LPS/Sham, and LPS/Dexamethasone with LPS/Sham as a pharmacological control.

For MPO activity, cytokine expression (RT-qPCR), and histopathology, a one-way ANOVA was used with Group (six levels) as the factor (yielding statistics such as F(5,66)), followed by Bonferroni post hoc tests with the same primary contrasts.

To assess the safety of PBM in healthy lungs, a separate one-way ANOVA compared vehicle groups (Vehicle/Sham, Vehicle/LED 430 nm, Vehicle/Laser 660 nm, Vehicle/Laser 808 nm). No significant differences were observed ($P > 0.05$); detailed data are available in Supplementary Table S1 . Results are expressed as mean ± SEM, and significance was set at $P < 0.05$. Analyses were conducted using GraphPad Prism 6.0.

## Results

All experimental groups were analyzed relative to their respective controls (PBS), with assessments conducted at baseline (BL) and 24 hours after LPS instillation.

### *Respiratory Mechanics*

The two-way repeated-measures ANOVA revealed significant main effects of Group and Time, as well as a Group × Time interaction ($P < 0.001$) for all ventilatory mechanics variables — airway resistance (Raw, Figure 1), tissue viscosity (Gtis, Figure 2), tissue elastance (Htis, Figure 3), and hysteresis (η, Figure 4). Bonferroni post hoc comparisons showed that LPS/Sham animals exhibited marked increases in all parameters compared to PBS/Sham ($P < 0.001$), indicating impaired lung mechanics following injury. Treatment with the 660-nm laser significantly reduced Raw ($P < 0.01$), Gtis ($P < 0.05$), Htis ($P < 0.001$), and η ($P < 0.05$) compared to LPS/Sham, restoring these values to levels statistically similar to those observed with dexamethasone ($P > 0.05$ vs. LPS/DEXA).

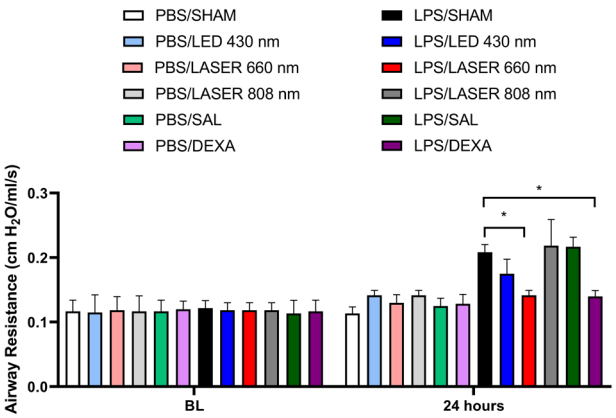


**Figure 1.** Effects of photobiomodulation on airway resistance (Raw) in rats with LPS-induced acute lung injury. Data are shown at baseline (BL) and 24 hours after LPS or vehicle instillation for the following groups: PBS/SHAM, PBS/LED 430 nm, PBS/LASER 660 nm, PBS/LASER 808 nm, PBS/SAL, PBS/DEXA, LPS/SHAM, LPS/LED 430 nm, LPS/LASER 660 nm, LPS/LASER 808 nm, LPS/SAL, and LPS/DEXA. LPS significantly increased airway resistance, whereas treatment with the 660 nm laser reduced this parameter, with effects comparable to dexamethasone. Data are expressed as mean ± SEM.

In contrast, neither the 808-nm laser nor the 430-nm LED produced significant improvements in any ventilatory parameters ($P > 0.05$), confirming that the 660-nm wavelength was the only phototherapy capable of effectively restoring lung mechanics.

### *Myeloperoxidase (MPO) Activity*

A one-way ANOVA revealed a significant effect of Group on MPO activity ($F(5,66) \approx 12.4$, $P < 0.0001$; Figure 5). LPS instillation markedly increased MPO activity compared to PBS/Sham ($P < 0.001$). Treatment with the 660-nm laser significantly reduced MPO levels relative to LPS/Sham ($P < 0.01$), reaching values comparable to those observed with dexamethasone ($P > 0.05$ vs. LPS/DEXA). In contrast, the 808-nm laser and 430-nm LED did not produce significant reductions ($P > 0.05$), indicating a selective anti-inflammatory effect for the red-light (660 nm) laser treatment.

### *Cytokine Expression (RT-qPCR)*

Analysis of cytokine mRNA expression (Figure 6) revealed significant treatment effects for TNF-α ($F_{5,66} \approx 15.7$, $p < 0.0001$), IL-6 ($F_{5,66} \approx 11.2$, $p < 0.0001$), IL-1β ($F_{5,66} \approx 9.5$, $P < 0.001$), and IL-10 ($F_{5,66} \approx 8.3$, $P < 0.001$). TNF-α and IL-6 expression levels were significantly elevated in LPS/sham compared with PBS ($P < 0.001$). Treatment with the 430-nm LED, 660-nm laser, and 808-nm laser

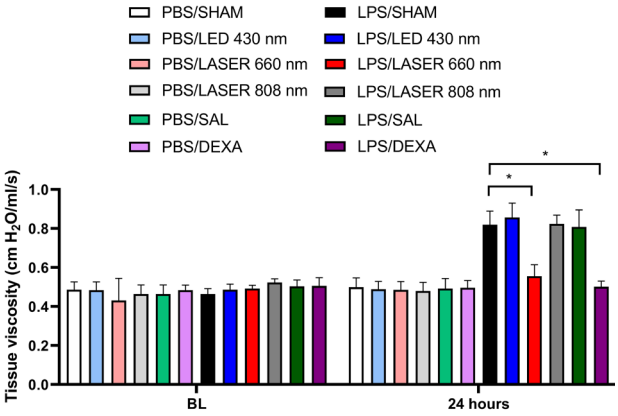


Figure 2. Effects of photobiomodulation on tissue viscosity (Gtis) in rats with LPS-induced acute lung injury. Measurements were obtained at baseline (BL) and 24 hours after experimental induction. LPS increased tissue viscosity compared with control animals, and treatment with the 660 nm laser significantly attenuated this increase. Neither the 430 nm LED nor the 808 nm laser significantly improved this parameter. Data are expressed as mean ± SEM.

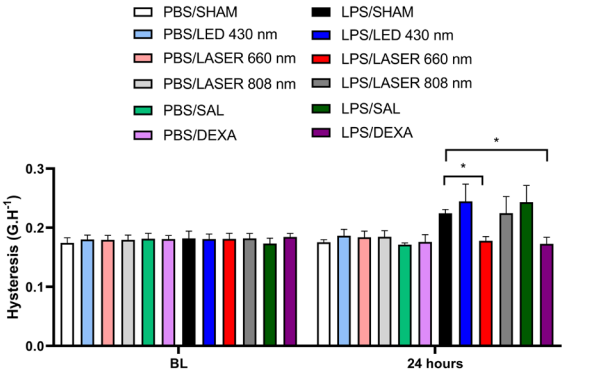


**Figure 4.** Effects of photobiomodulation on hysteresivity (η) in rats with LPS-induced acute lung injury. Values were assessed at baseline (BL) and 24 hours after lung injury induction. LPS significantly increased hysteresivity, while the 660 nm laser reduced this alteration. The 430 nm LED and 808 nm laser did not significantly improve this variable. Data are expressed as mean ± SEM.

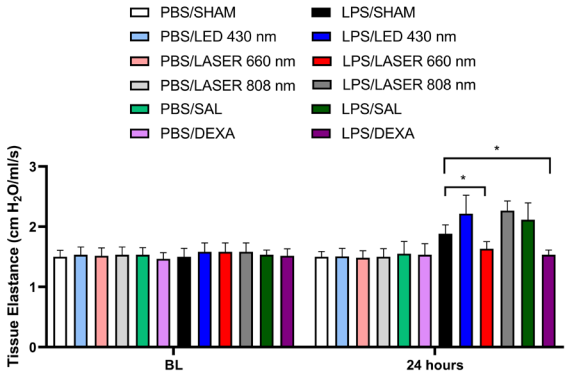


**Figure 3.** Effects of photobiomodulation on tissue elastance (Htis) in rats with LPS-induced acute lung injury. Measurements were performed at baseline (BL) and 24 hours after LPS or vehicle instillation. LPS caused a marked increase in tissue elastance, indicating impaired pulmonary mechanics. Treatment with the 660 nm laser significantly reduced elastance, with results similar to those observed in the dexamethasone group. Data are expressed as mean ± SEM.

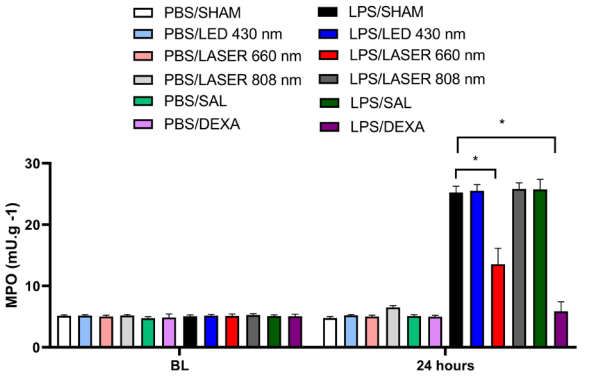


**Figure 5.** Effects of photobiomodulation on myeloperoxidase (MPO) activity in lung tissue 24 hours after LPS-induced acute lung injury. LPS markedly increased MPO activity, reflecting neutrophil recruitment and pulmonary inflammation. Treatment with the 660 nm laser significantly reduced MPO activity, with values approaching those observed in the dexamethasone-treated group. Data are expressed as mean ± SEM.

each significantly reduced TNF-α and IL-6 expression ($P<0.05$ to $P<0.001$ vs. LPS/sham). For IL-1β and IL-10, only the 430-nm LED and 660-nm laser significantly decreased expression compared with LPS/sham ($P<0.05$), whereas the 808-nm laser did not produce significant effects ($P>0.05$).

Importantly, the reduction of pro-inflammatory markers by the 660-nm laser was consistent across all cytokines analyzed, closely approximating the anti-inflammatory profile observed with dexamethasone (Figure 3).

### *Histopathology*

Histological analysis supported the functional and molecular findings. Control lungs (PBS) displayed preserved alveolar structures, with thin septa and absence of infiltrates. LPS/sham animals showed extensive pathological changes, including neutrophil infiltration in alveolar capillaries, interstitial edema, and epithelial cell injury (Figure 7).

Treatment with the 660-nm red laser markedly attenuated these alterations, showing reduced neutrophil accumulation and preservation of alveolar integrity. The 808-nm laser produced partial histological improvement, consistent with its effect on TNF-α and IL-6, but without an impact on IL-1β or ventilatory mechanics. The 430-nm LED group showed minimal histological benefit, with persistent neutrophil infiltration and edema. Dexamethasone, as expected, robustly reduced inflammatory changes.

### *Vehicle/PBM safety evaluation*

Animals treated with photobiomodulation in the absence of LPS (vehicle/LED, vehicle/laser 660 nm, vehicle/laser

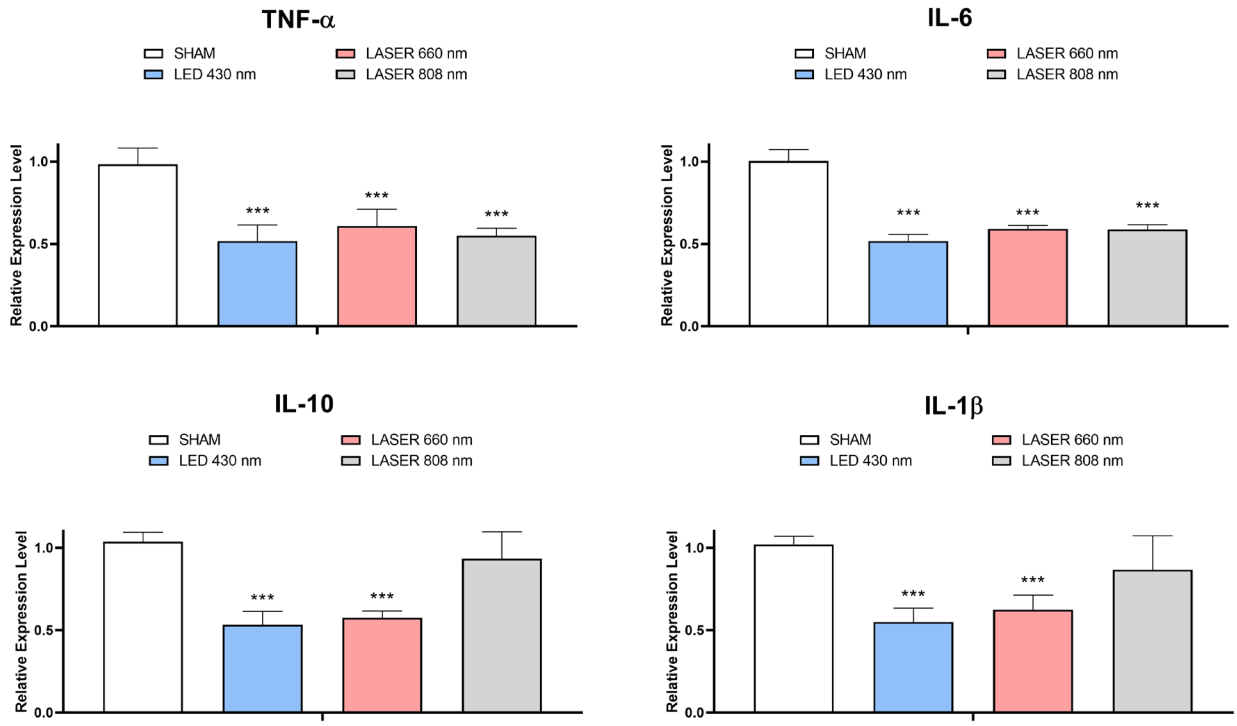


**Figure 6.** Effects of photobiomodulation on pulmonary cytokine expression in rats with LPS-induced acute lung injury. Relative mRNA expression of TNF-**α**, IL-6, IL-10, and IL-1**β** was determined by RT-qPCR in lung tissue collected 24 hours after injury induction. LPS increased the expression of inflammatory cytokines, whereas the 660 nm laser reduced all cytokines analyzed. The 430 nm LED also reduced selected cytokines, while the 808 nm laser showed a more limited effect. Data are expressed as relative expression normalized to the control group.

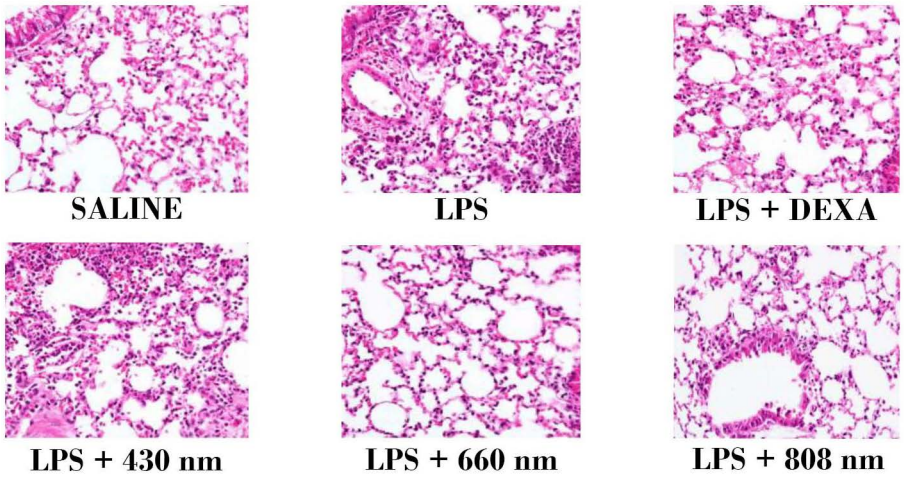


**Figure 7.** Representative histological sections of lung tissue stained with hematoxylin and eosin from saline, LPS, LPS + dexamethasone, LPS + 430 nm LED, LPS + 660 nm laser, and LPS + 808 nm laser groups. The LPS group showed inflammatory cell infiltration, alveolar wall thickening, and edema. Treatment with the 660 nm laser attenuated these histopathological alterations, whereas the 808 nm laser showed partial improvement and the 430 nm LED showed minimal histological benefit.

808 nm) showed ventilatory mechanics, MPO activity, and cytokine expression comparable to those of the vehicle/sham group ($P > 0.05$ for all variables). Histological analysis also revealed preserved alveolar architecture without neutrophil infiltration or edema, confirming that the phototherapies alone did not induce detectable inflammatory or structural changes in healthy lungs.

The detailed data for vehicle/PBM groups are provided in Supplementary Table S1.

## Discussion

In this study, photobiomodulation demonstrated wavelength-dependent effects in a rat model of LPS-induced acute lung injury. The 660 nm red laser significantly improved ventilatory mechanics, reduced myeloperoxidase activity, and downregulated key inflammatory cytokines (TNF-α, IL-6, IL-1β, and IL-10), with histological evidence of attenuated neutrophil infiltration and alveolar edema—results comparable to

dexamethasone. The 430-nm LED showed partial anti-inflammatory activity, reducing selected cytokines but without functional or histological improvement, while the 808-nm infrared laser reduced only TNF-α and IL-6 and provided modest histological protection, without effects on respiratory mechanics. Taken together, these findings indicate that the 660-nm wavelength exerts the most consistent and robust protective effects against lung injury, supporting its potential as an adjuvant therapeutic strategy for ALI/ARDS.

Application of PBM to the lung markedly influenced both local and systemic inflammatory responses. Previous reports indicate that PBM not only reduces pulmonary inflammation but also attenuates systemic inflammatory activity, thereby improving ventilatory mechanics, particularly in hypoxic tissues.[20,21] Our results are consistent with these findings, suggesting that PBM is especially promising in the context of ALI/ARDS, where gas exchange is severely compromised.[22]

In the present study, treatment with the 660 nm red laser significantly reduced airway resistance, tissue elastance, viscosity, and hysteresis, in parallel with reductions in MPO activity and pro-inflammatory cytokines. These findings corroborate the work of Oliveira et al[23], who demonstrated suppression of the inflammatory process and regenerative effects of PBM in pulmonary models. Similarly, De Lima et al.[24] showed a reduction in acute lung inflammation with light therapy, aligning with the positive outcomes we observed for the 660 nm laser. Oliveira et al. also reported attenuation of ARDS severity in mice following PBM, reinforcing the therapeutic potential of this approach.[15]

Nejatifard et al.[15] highlighted that PBM reduces pulmonary edema, cytokine levels in bronchoalveolar lavage fluid, neutrophil influx, and MPO activity. Consistent with this, our study demonstrated that the 660 nm red laser and dexamethasone significantly decreased MPO activity, whereas the 808 nm infrared laser and 430 nm LED showed only partial or absent effects. Histological analysis confirmed these outcomes, with visible attenuation of neutrophilic infiltration and alveolar edema in the 660 nm and dexamethasone groups.

Cytokine analysis further supported these findings. LPS instillation led to a robust increase in TNF-α, IL-6, IL-1β, and IL-10, consistent with the cytokine storm observed in ALI/ARDS.[25] Treatment with the 660 nm laser and 430 nm LED reduced all four markers, while the 808 nm infrared laser only reduced TNF-α and IL-6, without significant effects on IL-1β or IL-10. The molecular effects observed here align with the cellular mechanisms described by Nejatifard et al[15], where PBM acts at molecular, cellular, and tissue levels to counteract excessive inflammation and promote tissue regeneration.

Our results also corroborate previous findings by De Lima et al.[24] and Oliveira et al.[23], who demonstrated that PBM decreases TNF-α expression, reduces alveolar macrophage activation, and limits neutrophil migration into lung tissue—key mechanisms in ARDS pathogenesis. Importantly, these effects appear wavelength-dependent: red light lasers (650–660 nm) are frequently reported to achieve better penetration into lung tissue and to yield superior anti-inflammatory outcomes.[15,26] This is consistent with our data, as significant improvements in ventilatory mechanics and cytokine modulation were observed only in the 660 nm group.

By contrast, infrared lasers (808–830 nm) have shown anti-inflammatory potential in other contexts.[15,25,27] Kingsley et al.[27] reported viral inactivation across wavelengths, but our data do not support strong efficacy for the 808 nm laser in ALI/ARDS, as we did not observe reductions in ventilatory impairment or broad cytokine modulation. One possible explanation, as suggested by Sabino et al.[21], is that light penetration in small animals is more effective than in humans; thus, in our rat model, the 808 nm wavelength may have surpassed the lesion depth, limiting its efficacy in inflamed tissue.

The superior efficacy of the 660 nm red laser observed in this study likely reflects wavelength-specific interactions between light and biological chromophores, particularly mitochondrial cytochrome c oxidase (CCO), which exhibits major absorption peaks in the red (≈630–670 nm) and near-infrared (≈800–840 nm) ranges.[15,16] Absorption of 660 nm photons by CCO promotes enhanced electron transport and mitochondrial membrane potential, leading to increased ATP synthesis and the controlled release of reactive oxygen species (ROS) that act as secondary messengers to modulate NF-κB and other inflammatory transcription factors.[15,21] In immune and epithelial cells, this mechanism can suppress excessive cytokine production and neutrophil activation, consistent with the broad down-regulation of TNF-α, IL-6, and IL-1β observed here.

While the present results suggest a wavelength-dependent pattern of efficacy, differences in fluence and irradiance among emitters may also contribute to the observed outcomes. Blue light requires higher radiant exposure to reach comparable photon delivery at depth, whereas red and near-infrared lasers achieve higher irradiance but over smaller areas.[15,17,21] These physical differences affect energy distribution, penetration, and chromophore activation, potentially interacting with wavelengths to shape the overall biological effect. Therefore, our conclusion of "wavelength dependence" should be interpreted within the context of dose- and irradiance-related factors, and future work should include dose-response and area-matched protocols to disentangle these variables and optimize PBM parameters for lung inflammation.[23,24]

Additionally, optical penetration characteristics may contribute to the wavelength-dependent effects. Red light

(660 nm) achieves an optimal balance between photon absorption and scattering in biological tissue, enabling efficient energy deposition within the superficial and mid-parenchymal lung layers, where inflammatory infiltrates predominate in LPS-induced injury. By contrast, shorter wavelengths (430 nm) are strongly absorbed by hemoglobin and rapidly attenuated, while longer near-infrared wavelengths (808 nm) penetrate more deeply but may surpass the effective target depth in small-animal lungs, dissipating energy beyond inflamed regions.[17,21] These combined biophysical and biochemical factors likely explain the efficacy of gradients observed among the tested wavelengths and support the preferential use of 660 nm light for modulating acute pulmonary inflammation.

Although IL-10 is classically anti-inflammatory, its upregulation during ALI/ARDS is tightly coupled to the same upstream stimuli that drive TNF-α and IL-6. When PBM mitigates the early inflammatory trigger, both pro- and counter-regulatory mediators can decline concurrently, reflecting a global normalization of the cytokine network rather than a pro-inflammatory shift. In this context, the decrease in IL-10 after PBM likely mirrors a reduced need for counter-regulation once the inflammatory drive is blunted.[9,4,15,23,24] Future work should include time-course and protein-level analyses to characterize the overall IL-10/TNF-α balance over time.

It is important to contextualize the between-device comparisons by considering beam geometry and power density. Although we targeted a similar energy scale across devices, the lasers delivered substantially higher irradiance and radiant exposure over a smaller spot (e.g., 150 J/cm² at 1.67 W/cm² for 660/808 nm) than the LED (27 J/cm² at 0.90 W/cm²). Differences in coherence, divergence, and spectral bandwidth between lasers and LEDs, coupled with wavelength-dependent absorption/scattering in lung tissue (the "optical window"), likely influenced photon distribution and biological activation of mitochondrial chromophores (e.g., cytochrome-c oxidase) and downstream inflammatory signaling.[15,17] Thus, while the 660 nm laser showed the most consistent efficacy across functional, molecular, and histological endpoints, these results should be interpreted as qualitative device-level comparisons rather than strictly dose-equivalent effects; future work should include dose–response and area-matched protocols to harmonize radiant exposure and irradiance across emitters.

Altogether, these findings indicate that while multiple wavelengths exert partial anti-inflammatory effects, only the 660 nm red laser consistently reduced ventilatory dysfunction, MPO activity, and the full spectrum of cytokine alterations, with histological evidence of attenuated lung injury. This wavelength appears to offer the most robust therapeutic profile among the PBM protocols tested in the LPS-induced lung injury model.

## Conclusion

Photobiomodulation demonstrated wavelength-dependent effects in a rat model of LPS-induced acute lung injury. Among the tested interventions, the 660 nm red laser was the only modality capable of consistently improving ventilatory mechanics, reducing myeloperoxidase activity, and modulating the full spectrum of inflammatory cytokines, with corroborating histological evidence of attenuated lung injury. In contrast, the 430 nm LED and 808 nm infrared laser produced partial and limited effects, respectively, without restoring pulmonary function. These findings indicate that red-light photobiomodulation (660 nm) provides the most robust anti-inflammatory and functional benefits in this model and may represent a promising adjunctive therapeutic strategy for acute lung inflammation. Further studies are warranted to optimize dosimetry and to evaluate translational applicability in clinical settings.

### Authors' Contribution

Conceptualization: Gabrielly Santos Pereira; Marcelo Lourenço da Silva.
Data curation: Rafaella Rocha Figueiredo; Gabrielly Santos Pereira; Laura Pereira Generoso; Josie Resende Torres da Silva; João Eduardo de Araújo; Marcelo Lourenço da Silva.
Formal analysis: Gabrielly Santos Pereira; João Eduardo de Araújo; Marcelo Lourenço da Silva.
Investigation: Rafaella Rocha Figueiredo; Gabrielly Santos Pereira; Laura Pereira Generoso; Marcelo Lourenço da Silva.
Methodology: Gabrielly Santos Pereira; João Eduardo de Araújo; Josie Resende Torres da Silva; Marcelo Lourenço da Silva.
Project administration: Marcelo Lourenço da Silva.
Resources: Marcelo Lourenço da Silva.
Software: João Eduardo de Araújo; Marcelo Lourenço da Silva.
Supervision: João Eduardo de Araújo; Marcelo Lourenço da Silva.
Validation: João Eduardo de Araújo; Marcelo Lourenço da Silva.
Visualization: Rafaella Rocha Figueiredo; Gabrielly Santos Pereira; Laura Pereira Generoso; Josie Resende Torres da Silva; Marcelo Lourenço da Silva.
Writing – original draft: Gabrielly Santos Pereira; Rafaella Rocha Figueiredo; Laura Pereira Generoso; Josie Resende Torres da Silva; Marcelo Lourenço da Silva.
Writing – review & editing: Gabrielly Santos Pereira; Rafaella Rocha Figueiredo; Laura Pereira Generoso; João Eduardo de Araújo; Josie Resende Torres da Silva; Marcelo Lourenço da Silva.

### Competing Interests

The authors declare no conflict of interest.

### Data Availability of Statement

Data will be made available on request.

### Ethical Approval

All experimental procedures involving animals were conducted in strict accordance with the ethical guidelines for the care and use of laboratory animals established by the Federal University of Alfenas (UNIFAL-MG). The study protocol was reviewed and approved by the Institutional Animal Care and Use Committee (IACUC) under protocol number 21/2020. Efforts were made to minimize animal suffering and to use the minimum number of animals necessary to obtain reliable results.

**Funding**
This study was supported by the Coordenação de Aperfeiçoamento de Pessoal de Nível Estado de Minas Gerais (FAPEMIG). GSP and LPG received a FAPEMIG scholarship as part of this research. RCF received a CAPES scholarship as part of this research.

**Supplementary Files**
Supplementary file 1 contains Table S1.

**References**
1. Matthay MA, Zimmerman GA, Esmon C, Bhattacharya J, Coller B, Doerschuk CM, et al. Future research directions in acute lung injury: summary of a National Heart, Lung, and Blood Institute working group. Am J Respir Crit Care Med 2003;167(7):1027–35. doi:10.1164/rccm.200208-966WS
2. Savin IA, Zenkova MA, Sen'kova AV. Pulmonary Fibrosis as a Result of Acute Lung Inflammation: Molecular Mechanisms, Relevant In Vivo Models, Prognostic and Therapeutic Approaches. Int J Mol Sci 2022;23(23). doi:10.3390/ijms232314959
3. D'Alessio FR. Mouse Models of Acute Lung Injury and ARDS. Methods Mol Biol 2018;1809:341–50. doi:10.1007/978-1-4939-8570-8_22
4. Matute-Bello G, Downey G, Moore BB, Groshong SD, Matthay MA, Slutsky AS, et al. An official American Thoracic Society workshop report: features and measurements of experimental acute lung injury in animals. Am J Respir Cell Mol Biol 2011;44(5):725–38. doi:10.1165/rcmb.2009-0210ST
5. Beck-Schimmer B, Schwendener R, Pasch T, Reyes L, Booy C, Schimmer RC. Alveolar macrophages regulate neutrophil recruitment in endotoxin-induced lung injury. Respir Res 2005;6(1):61. doi:10.1186/1465-9921-6-61
6. Fusco LB, PÊGo-Fernandes PM, Xavier AM, Pazetti R, Rivero DHRF, Capelozzi VL, et al. Modelo experimental de enfisema pulmonar em ratos induzido por papaína. J. Pneumologia 2002;28(1):1-7. doi:https://doi.org/10.1590/S0102-35862002000100003
7. Beck-Schimmer B, Schwendener R, Pasch T, Reyes L, Booy C, Schimmer RC. Alveolar macrophages regulate neutrophil recruitment in endotoxin-induced lung injury. Respir Res 2005;6(1):61. doi:10.1186/1465-9921-6-61
8. Fan EKY, Fan J. Regulation of alveolar macrophage death in acute lung inflammation. Respir Res 2018;19(1):50. doi:10.1186/s12931-018-0756-5
9. Matthay MA, Zemans RL, Zimmerman GA, Arabi YM, Beitler JR, Mercat A, et al. Acute respiratory distress syndrome. Nat Rev Dis Primers 2019;5(1):18. doi:10.1038/s41572-019-0069-0
10. Sathe NA, Mostaghim A, Barnes E, O'Connor NG, Sahi SK, Sakr SS, et al. Biomarker Signatures of Severe Acute Kidney Injury in a Critically Ill Cohort of COVID-19 and Non-COVID-19 Acute Respiratory Illness. Crit Care Explor 2023;5(7):e0945. doi:10.1097/cce.0000000000000945
11. Liu C, Xiao K, Xie L. Advances in the use of exosomes for the treatment of ALI/ARDS. Front Immunol 2022;13:971189. doi:10.3389/fimmu.2022.971189
12. Enwemeka CS, Bumah VV, Masson-Meyers DS. Light as a potential treatment for pandemic coronavirus infections: A perspective. J Photochem Photobiol B 2020;207:111891. doi:10.1016/j.jphotobiol.2020.111891
13. Ye R, Liu Z. ACE2 exhibits protective effects against LPS-induced acute lung injury in mice by inhibiting the LPS-TLR4 pathway. Exp Mol Pathol 2020;113:104350. doi:10.1016/j.yexmp.2019.104350
14. Page MJ, Kell DB, Pretorius E. The Role of Lipopolysaccharide-Induced Cell Signalling in Chronic Inflammation. Chronic Stress (Thousand Oaks) 2022;6:24705470221076390. doi:10.1177/24705470221076390
15. Nejatifard M, Asefi S, Jamali R, Hamblin MR, Fekrazad R. Probable positive effects of the photobiomodulation as an adjunctive treatment in COVID-19: A systematic review. Cytokine 2021;137:155312. doi:10.1016/j.cyto.2020.155312
16. de Oliveira Martins D, Martinez dos Santos F, Evany de Oliveira M, de Britto LR, Benedito Dias Lemos J, Chacur M. Laser therapy and pain-related behavior after injury of the inferior alveolar nerve: possible involvement of neurotrophins. J Neurotrauma 2013;30(6):480–6. doi:10.1089/neu.2012.2603
17. Ash C, Dubec M, Donne K, Bashford T. Effect of wavelength and beam width on penetration in light-tissue interaction using computational methods. Lasers Med Sci 2017;32(8):1909–18. doi:10.1007/s10103-017-2317-4
18. Sahu KK, Mishra AK, Lal A. Coronavirus disease-2019: An update on third coronavirus outbreak of 21st century. Qjm 2020;113(5):384–6. doi:10.1093/qjmed/hcaa081
19. Reutershan J, Basit A, Galkina EV, Ley K. Sequential recruitment of neutrophils into lung and bronchoalveolar lavage fluid in LPS-induced acute lung injury. Am J Physiol Lung Cell Mol Physiol 2005;289(5):L807–L815. doi:10.1152/ajplung.00487.2004
20. Pereira PC, de Lima CJ, Fernandes AB, Zângaro RA, Villaverde AB. Cardiopulmonary and hematological effects of infrared LED photobiomodulation in the treatment of SARS-COV2. J Photochem Photobiol B 2023;238:112619. doi:10.1016/j.jphotobiol.2022.112619
21. Sabino CP, Ball AR, Baptista MS, Dai T, Hamblin MR, Ribeiro MS, et al. Light-based technologies for management of COVID-19 pandemic crisis. J Photochem Photobiol B 2020;212:111999. doi:10.1016/j.jphotobiol.2020.111999
22. Caputo ND, Strayer RJ, Levitan R. Early Self-Proning in Awake, Non-intubated Patients in the Emergency Department: A Single ED's Experience During the COVID-19 Pandemic. Acad Emerg Med 2020;27(5):375–8. doi:10.1111/acem.13994
23. Oliveira MC, Jr., Greiffo FR, Rigonato-Oliveira NC, Custódio RW, Silva VR, Damaceno-Rodrigues NR, et al. Low level laser therapy reduces acute lung inflammation in a model of pulmonary and extrapulmonary LPS-induced ARDS. J Photochem Photobiol B 2014;134:57–63. doi:10.1016/j.jphotobiol.2014.03.021
24. de Lima FM, Moreira LM, Villaverde AB, Albertini R, Castro-Faria-Neto HC, Aimbire F. Low-level laser therapy (LLLT) acts as cAMP-elevating agent in acute respiratory distress syndrome. Lasers Med Sci 2011;26(3):389–400. doi:10.1007/s10103-010-0874-x
25. Soheilifar S, Fathi H, Naghdi N. Photobiomodulation therapy as a high potential treatment modality for COVID-19. Lasers Med Sci 2021;36(5):935–8. doi:10.1007/s10103-020-03206-9
26. Sigman SA, Mokmeli S, Vetrici MA. Adjunct low level laser therapy (LLLT) in a morbidly obese patient with severe COVID-19 pneumonia: A case report. Can J Respir Ther 2020;56:52–6. doi:10.29390/cjrt-2020-022
27. Kingsley D, Kuis R, Perez R, Basaldua I, Burkins P, Marcano A, et al. Oxygen-dependent laser inactivation of murine norovirus using visible light lasers. Virol J 2018;15(1):117. doi:10.1186/s12985-018-1019-2